NUCLEAR INSTRUMENTS AND METHODS 26 (1964) 274–284; © NORTH-HOLLAND PUBLISHING CO.

HIGH RESOLUTION SECOND DIFFERENCE ANALYSIS OF PHOTONUCLEAR YIELD CURVES

K. N. GELLER and E. G. MUIRHEAD

*Physics Department, University of Pennsylvania Philadelphia 4, Pennsylvania**

Received 30 August 1963

A critical evaluation of the problems involved in the high resolution analysis of photonuclear cross sections from bremsstrahlung yield curves is presented. In particular, the effect of the analysis bin width and the shape of the x-ray spectrum are considered. A method is presented which circumvents the need to know the shape of the spectrum at the high energy tip; the latter information is contained in an effective energy resolution function that does not enter in the analysis, but for a normalization factor. The method, which is an iterative one, is based on taking the second difference of the photonuclear yield curve and is applicable to measurements made with bremsstrahlung in energy intervals less than 200 keV. An analytic smoothing procedure is used. The satisfactory performance of the method is demonstrated by the analysis of three synthesized yield curves.

1. Introduction

A large body of our experimental knowledge about photonuclear processes come from studies undertaken with the continuous radiation spectrum produced in electron bremsstrahlung. The structure of these experiments precludes any direct measurement of the cross section of the photo-nuclear process under investigation. Instead, these experiments measure a quantity proportional to the bremsstrahlung weighted cross section or more commonly the integral yield per unit of monitor response. Measuring the integral yield at various values of the maximum energy of the bremsstrahlung beam generates a yield curve, and the reaction cross section is then deduced from this yield curve, assuming that the radiation spectrum for the experimental situation is known.

The various procedures which have been proposed to calculate the cross section from the measured yield data are straightforward and discussed extensively in the literature[1]). Although the cross section computed by these analytical methods is unique, identification with the physical cross section presumes a detailed knowledge of the yield function and the experimental radiation spectrum. In practice, neither the yield function nor the spectrum is known exactly. Invariably, the yield function is known only to a reasonable degree of precision and only at a series of beam energies (K_0), usually separated by equal energy intervals, say Δ (bin width). Hence, the cross section deduced from each measurement is some kind of weighted average over the energy interval Δ, where Δ is a measure of the experimental energy resolution.

Now, aside from energy resolution considerations, any difference between the assumed and actual radiation spectra will be reflected in the values computed for the cross section. The effect of a spectrum change on this computed cross section will depend on the extent of the disagreement between assumed and actual spectra, on the energy resolution, and on the true variation of the reaction cross section with energy. Generally speaking, in most experiments using bremsstrahlung, the energy resolution is nominally $\frac{1}{4}$MeV or greater and only the gross structure of the reaction cross section in the giant resonance region has been extracted. However, when the photoreaction cross section is characterized by discrete resonances having widths of the order of several tens of keV and level separations of several hundreds of keV, an energy resolution comparable to or less than the level widths is called for. Under such circumstances the effect of a spectrum modification can be very great[1,2]). Hence, in order to compute the cross section where sharp resonances are involved, the radiation spectrum incident on the sample must be known quite accurately. The common practice of assuming a radiation spectrum given by the extreme relativistic Born approximation calculation (the so-called Schiff spectrum[3])) is no longer suitable. The thin-target or "intrinsic" bremsstrahlung spectrum must now be replaced by the appropriate thick-target spectrum.† Modification of the intrinsic spectrum produced by electron energy loss, electron scattering in the radiator, and by the energy dispersion of the primary electrons striking the radiator must be considered. The problem is complicated still further by the dependence of the bremsstrahlung cross section on

* Supported in part by the Office of Naval Research, the Air Force Research and Development Command, and the National Science Foundation.

† For this discussion a thick-target may be defined as one for which multiple electron scattering effects are important but which is still very much smaller than the range corresponding to the incident electron energy.

1) A. S. Penfold and J. Leiss, Phys, Rev. **114** (1959) 1332.
2) A. S. Penfold and B. M. Spicer, Phys. Rev. **100** (1955) 1377.
3) L. I. Schiff, Phys. Rev. **83** (1951) 252.

the photon emission angle[3]). Consequently, the spectrum shape is influenced, albeit slightly by the angle subtended by the nuclear target at the radiator. For activation experiments, this acceptance angle determines an effective X-ray target thickness somewhat greater than the geometrical thickness of the radiator. A procedure for evaluating the thick-target spectrum in terms of the intrinsic spectrum is available[4]), but has not been widely used since the detailed shape of the bremsstrahlung spectrum in the immediate vicinity of the high energy tip has not been satisfactorily predicted[5]). Consequently, high resolution cross section analysis of bremsstrahlung yield data by conventional techniques has not been attempted over a large energy region.

Up to the present, fine structure in photo reaction cross sections has been inferred from two main types of experiment. Where the reaction products are charged particles, these have been recorded in nuclear emulsions. These experiments suffer from the limitations imposed by statistical accuracy and energy resolution, the latter being in general several hundred keV for protons. Activation experiments on the other hand give a well-defined yield curve from which fine structure has often been successfully inferred from relatively sharp changes in curvature of the yield curve. From this procedure are obtained the so-called *breaks* which first indicated the extent of level absorption in oxygen, carbon and other light nuclei. It is now realized that this approach can only provide unambiguous information about level structure in restricted situations, viz., in the region of a few million electron volts above the reaction threshold. For the determination of structure in the giant resonance region, there is no substitute for a complete cross section analysis such as the one to be described below.

In view of the above mentioned difficulties we have developed a new method for the analysis of high resolution bremsstrahlung yield data which has significant advantages over previous methods. For the latter it is essential to know exactly the relative number of photons in each energy bin right to the high energy tip of the spectrum. A significant error in this number for the uppermost bin, for example, produces a correspondingly serious error in the computed cross section. In the present method, which is an iterative one, this difficulty is overcome by replacing the detailed shape *at the tip* by an effective resolution function, based on the variation of the spectrum with energy over several bins *in the tip vicinity*. Since the integrated area rather than the detailed shape of this effective resolution function is of primary significance in the subsequent cross section analysis, the exact shape is not required at the spectral tip. A sufficiently precise estimate of this shape may be inferred from a knowledge of the expected behaviour of a thick target spectrum in this region, together with an experimental measurement of this spectrum, even though the latter is almost always of limited statistical accuracy owing to the inherent difficulty of the measurement. At photon energies removed from the tip, the shape is assumed proportional to the theoretical bremsstrahlung cross section.

The general principles of the present second-difference method (s.d.m.) have already been published by Geller[6]). The s.d.m. involves the calculation of second differences of the yield and spectrum functions. It is applicable to photonuclear yield curves measured with thick-target bremsstrahlung in energy intervals less than the energy loss equivalent of the bremsstrahlung target thickness (approximately 200 keV). It has been used to produce the $O^{16}(\gamma,n)O^{15}$ cross section from threshold to 17.5 MeV in 34 keV steps, and from threshold to 23 MeV in 68 keV steps[7]).

In sec. 2 a brief outline of the general procedure of cross section analysis is summarized, followed by details of the second-difference method in sec. 3. In applying the s.d.m. to actual yield curves, it is desirable to damp out fluctuations due to statistical uncertainties. This is achieved by using an analytical smoothing procedure outlined in sec. 4. A test of the general procedure is discussed in sec. 5 where hypothetical yield curves are generated and subsequently analyzed allowing for the effects of statistics. In sec. 6 the photoneutron cross section for $O^{16}(\gamma,n)$ is presented.

2. Transformation Method of Cross Section Analysis

2.1. Introduction

In this section we review briefly the transformation method of cross section analysis originally proposed by Spencer[8]) and elaborated in a matrix formulation by Penfold and Leiss[1]). Although equivalent to the "total spectrum" and "photon difference" methods, the transformation method provides a clearer understanding of the problem and is fundamental to the present method.

The yield, Y, of a photonuclear reaction measured with electron bremsstrahlung extending to energy K_0 is related to the reaction cross section $\sigma(k)$ by the integral equation

4) A. S. Penfold, University of Illinois Report (unpublished).
5) E.g. the attempt of R. J. Jabbur and R. H. Pratt, Phys. Rev. **129** (1963) 184 and references herein.
6) K. N. Geller, Phys. Rev. **120** (1960) 2147.
7) K. N. Geller and E. G. Muirhead, Phys. Rev. Letters **11** (1963) 371.
8) L. V. Spencer, National Bureau of Standards Report, No. 1531, (Washington, D. C., 1952).

$$Y(K_0) = g\frac{\int_0^{K_0} \mathrm{d}k\sigma(k)\exp(-\mu_k x)N(k,K_0)}{\int_0^{K_0} \mathrm{d}kM(k)\exp(-\mu_k x')N(k,K_0)}$$
$$= (g/M(K_0))\int_0^{K_0} \mathrm{d}k\sigma(k)\exp(-\mu_k x)N(k,K_0)\,, \quad (1)$$

where $\sigma(k)$ is the cross section at energy k; $\exp(-\mu_k X)$ estimates the photon absorption in the radiator, sample and other material interposed between sample and radiator; g includes the target and efficiency factors; and $M(K_0)$, the monitor response function normalizes the spectrum $N(k,K_0)$. Instead of the number spectrum, $N(k,K_0)$, it is more convenient to use the corresponding intensity spectrum $\Phi(k,K_0)$ which is to a good approximation "shape-independent" for the energy range of K_0 used. Equation (1) is then to be solved for the *reduced cross section*

$$s(k) = \sigma(k)\exp(-\mu_k x)/k \quad (2)$$

according to the equation

$$y(K_0) = \int_0^{K_0} \mathrm{d}ks(k)\Phi(k,K_0)\,, \quad (3)$$

where the *reduced yield* $y(K_0) = Y(K_0)\cdot M(K_0)/g$.

Equation (3) can be solved exactly for $s(k)$ assuming that both the yield function and the radiation spectrum are known. Operate on both sides of eq.(3) with an appropriate transformation function $T(K_0,E_0)$ where $T=0$ for $K_0 > E_0$. T will be chosen so as to transform the spectrum to a δ-function spectrum*.

The relation between the *transformed yield* $\tilde{y}$ and the cross section is now prescribed by the *transformed spectrum* $\tilde{\Phi}$

$$\tilde{y}(E_0) = \int_0^{E_0} \mathrm{d}K_0 y(K_0)T(K_0,E_0)$$
$$= \int_0^{E_0} \mathrm{d}K_0 \int_0^{K_0} \mathrm{d}ks(k)\Phi(k,K_0)T(K_0,E_0)\,,$$

since $\Phi(k,K_0) = 0$ for $k > K_0$ we can write

$$\tilde{y}(E_0) = \int_0^{E_0} \mathrm{d}ks(k)\tilde{\Phi}(k,E_0)\,, \quad (4)$$

where the transformed spectrum $\tilde{\Phi}$ is defined by

$$\tilde{\Phi}(k,E_0) = \int_0^{E_0} \mathrm{d}K_0\Phi(k,K_0)T(K_0,E_0) \quad (5)$$

and merely expresses the fact that $\tilde{\Phi}$ is obtained by taking a linear combination of Φ's for various values of K_0. For a given $\tilde{\Phi}$, eq. (5) is solved for the transformation function $T(K_0,E_0)$. Thus for $\tilde{\Phi}(k,E_0) = \delta(E_0 - k)$ (delta function), the yield transformation immediately gives the reduced cross section, $s(E_0)$. In practice, eqs.(4) and (5) are solved numerically by matrix methods; T is then the inverse of the spectrum matrix for a delta function transformation.

2.2. Choice of spectrum

Now, the solution, $s(k)$, will differ from the true reduced cross section, $\Sigma(k)$, if the assumed spectrum does not correspond to the actual experimental situation. In practice, the intrinsic spectrum, $\varphi(k,K_0)$ is often used in place of the experimental spectrum $\Phi(k,K_0)$, and the transformation function $T(K_0,E_0)$ appropriate to $\varphi(k,K_0)$ is used to solve for $s(k)$. The departure of s from Σ depends on the nature of the spectrum generating function, $S(K_0',K_0)$ as defined by Penfold[4]), where $S(K_0',K_0) = 0$ for $K_0' > K_0$ and

$$\Phi(k,K_0) = \int_0^{K_0} \varphi(k,K_0')S(K_0',K_0)\,\mathrm{d}K_0'\,. \quad (6)$$

Operating on both sides of eq. (3) with $T(K_0,E_0)$ with Φ given by eq.(6) and $s(k)$ replaced by $\Sigma(k)$ we obtain†

$$\tilde{y}(E_0) = \int_0^{E_0} \mathrm{d}k\Sigma(k)\int_0^{E_0} \mathrm{d}K_0'\varphi(k,K_0')T_1(K_0',E_0)\,, \quad (7)$$

where the modified transformation function T_1 is given by

$$T_1(K_0',E_0) = \int_0^{E_0} \mathrm{d}K_0 S(K_0',K_0)T(K_0,E_0)\,. \quad (8)$$

The solution obtained using $\varphi(k,K_0)$ is given by

$$\tilde{y}(E_0) = \int_0^{E_0} \mathrm{d}ks(k)\tilde{\varphi}(k,E_0)\,, \quad (9)$$

where

$$\tilde{\varphi}(k,E_0) = \int_0^{E_0} \mathrm{d}K_0\varphi(k,K_0)T(K_0,E_0)\,.$$

Comparing eqs.7 and 9 with $\tilde{\varphi}$ a delta function we obtain

$$s(E_0) = \int_0^{E_0} \mathrm{d}k\Sigma(k)\int_0^{E_0} \mathrm{d}K_0'\varphi(k,K_0')T_1(K_0',E_0)\,. \quad (10)$$

Thus, the cross section computed with the intrinsic

* Other choices of T are possible, e.g. transformation to a spectrum $\tilde{N}(k,K_0) = \text{const.}$ leads to a solution for the integrated cross section.

† The effect of a spectrum change on the monitor response function is not very large and is not considered in the present discussion. For further details consult ref. 1.

spectrum is a weighted average of the true cross section $\Sigma(k)$. If thick-target effects are primarily responsible for the spectrum modification, then $S(K_0', K_0)$ spans a small energy range $K_0' - K_0 \simeq \delta$, where δ is a measure of the effective target thickness[4]). A large error will be introduced into the cross section computed with the intrinsic spectrum if the cross section exhibits sharp structure in an energy interval of order δ.

This is particularly true of light nuclei[2]), i.e. $A \leq 40$. In such cases the effect of a spectrum change is quite large.

3. Description of the Present Method

3.1. General discussion

In the previous section we showed that for the general transformation method a modification of the radiation spectrum in the immediate vicinity of the spectral tip can have a serious effect on the cross section computed from photonuclear yield data. Although the problem is solvable, given the modified thick-target radiation spectra, the computational labor involved in generating thick-target spectra is considerable.

Rather than proceed along these lines, we have developed a rather simple method of analysis which is not sensitive to the spectrum details in the immediate vicinity of the tip. Suppose in eq.(5) we separate the transformed spectrum $\tilde{\Phi}$ into two parts

$$\tilde{\Phi}(k, E_0) = \tilde{\Phi}_t(k, E_0) + \tilde{\Phi}_r(k, E_0), \qquad (11)$$

where $\tilde{\Phi}_t$ is equal to $\tilde{\Phi}$ for values of k in the immediate vicinity of the spectral tip, i.e. $k \simeq E_0$, and zero elsewhere; while $\tilde{\Phi}_r$ is zero in the immediate vicinity of the tip and equal to $\tilde{\Phi}$ at photon energies removed from the tip, i.e. $k < E_0$. Then, for any arbitrary transformation function, $T(K_0, E_0)$, only $\tilde{\Phi}_t$ is determined by the spectrum in the tip region. On substituting eq.(11), eq.(4) reduces to

$$\overline{s(k_t)} = s_0(E_0) - \int_0^{E_0} \frac{dk}{\Delta} s(k)\lambda(k, E_0, \Delta), \qquad (12)$$

where $\overline{s(k_t)}$ is the reduced cross section averaged over $\tilde{\Phi}_t(k, E_0)$

$$\overline{s(k_t)} = \int_0^{E_0} dk s(k)\tilde{\Phi}_t(k, E_0)/W(\Delta) \qquad (13a)$$

$$s_0(E_0) = \bar{y}(E_0)/W(\Delta) \qquad (13b)$$

$$\lambda(k, E_0, \Delta) = \Phi_r(k, E_0)\Delta/W(\Delta) \qquad (13c)$$

and

$$W(\Delta) = \int_0^{E_0} \Phi_t(k, E_0)\, dk \qquad (13d)$$

The explicit dependence of the residual term λ on bin width Δ will soon become apparent. Equation (12) can be solved by iteration for $\overline{s(k_t)}$ provided $\tilde{\Phi}_r$ is known. Since $\tilde{\Phi}_r$ is determined by the radiation spectrum at energies removed from the spectral tip, it can be calculated to sufficient accuracy for use here from the bremsstrahlung cross section given by Bethe-Heitler[9]) or Schiff[3]).

Now, if the $\overline{s(k_t)}$ computed from eqs.(13) is to bear some semblance to the actual cross section, then $\tilde{\Phi}_t(k, E_0)$ must assume the form of a suitable resolution function, say large and positive for values of k near E_0. The exact behavior of $\tilde{\Phi}$ of course, is determined by the transformation and the detailed shape of the spectrum near the tip. A detailed description of $\tilde{\Phi}_t$, however, is not necessary to calculate the average cross section. An empirical description of the spectrum tip shape is adequate to deduce the resolution function provided $\tilde{\Phi}$ goes to zero at the tip as is expected for a thick target spectrum.

3.2. Choice of transformation function

The choice of an appropriate transformation function is fundamental to the analysis. We require of the transformation that it be simple, generate a resolution function with desirable characteristics, and de-emphasize the contribution to $s(k)$ from the iterative term, i.e. $\lambda < 1$ for all values of k. The transformations we shall consider are the first and second difference of the radiation spectrum over an energy internal Δ. The transformed spectra $\Phi(k, E_0)$ or *weighting functions* are defined by

First difference weighting function (f.d.w.f.)

$$\Phi'(k, E_0, \Delta) = \Phi(k, E_0 + \tfrac{1}{2}\Delta) - \Phi(k, E_0 - \tfrac{1}{2}\Delta), \qquad (14a)$$

Second difference weighting function (s.d.w.f.)

$$\Phi''(k, E_0, \Delta) = \Phi(k, E_0 + \Delta) - 2\Phi(k, E_0) + \Phi(k, E_0 - \Delta) \qquad (14b)$$

The corresponding transformed yields are the first and second differences of the reduced yield, respectively. The dependence of each weighting function on E_0 and Δ is explicitly noted in eqs. (14). These functions are calculated for an intensity distribution of the simple form $\Phi(k, E_0) = A(E_0 - k)^n$ for $n = 0, 0.5$ and 1.0. The results, shown in fig. 1, are plotted as a function of $(E_0 - k)/\Delta$; thus plotted, each weighting function is found to be independent of E_0 and Δ. The actual spectrum, of course, will differ from these. However, in the immediate vicinity

[9]) H. Bethe and W. Heitler, Proc. Roy. Soc. (London) **A146** (1934) 83.

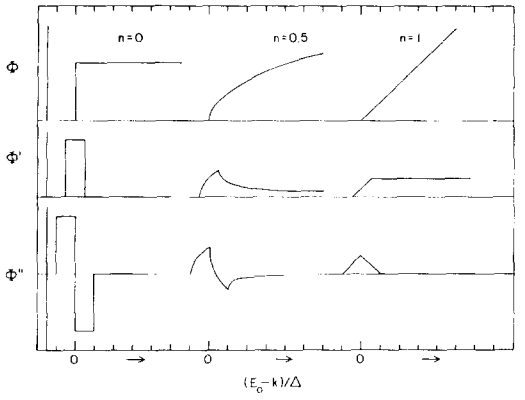

Fig. 1. Weighting functions for the bremstrahlung intensity distribution $\Phi = A_0(E\text{-}k)^n$ for $n = 0$, 0.5 and 1 as defined by (14a) and (14b).

of the spectral tip, the simple power law behavior is a close approximation to the actual target spectrum[10]).

We conclude from fig. 1 that if $0 \leq n < 0.5$, a first difference of the yield curve should approximate the actual cross section, whereas, for $0.5 < n \leq 1$, the second difference of the yield curve is to be preferred. For actual spectra, these conclusions will be modified by the dependence of each weighting function on bin width, Δ, particularly for large Δ.

[10]) H. W. Koch and J. W. Motz, Rev. Mod. Physics **31** (1959) 920.

The appropriate transformation for the analysis was deduced from the following considerations; (1) examination of the first and second difference of a representative yield curve measured in small energy intervals, and (2) an experimental determination of the spectrum isochromat at 15.12 MeV. The latter was measured by scattering photons elastically from the 15.12 MeV level of C^{12}.

In fig. 2 we show (a) the yield curve[7]) of the reaction $O^{16}(\gamma,n)O^{15}$ measured in energy intervals of 17 keV from threshold to 17.5 MeV; (b) the first difference of the yield curve for $\Delta = 68$ keV; and (c) the second difference of the yield curve for $\Delta = 68$ keV. Four independent sets of first and second difference curves are calculated from the interlaced sets of yield data. It is evident from fig. 2 that the second difference transformation is more appropriate than the first difference; the latter bears a closer resemblance to the integrated cross section. In neither case do we obtain the actual cross section or its integral, since the transformation we have used is only a first order approximation to the exact solution of the problem.

The conclusion drawn from the analyzed yield data is supported by our isochromat observation. The yield of 15.12 MeV photons scattered elastically at 120° from a carbon target is shown in fig. 3. A least squares fit of the yield data to $A(E_0 - k)^n$ (solid curve) gives a value of $n \simeq 0.6$. This result favors the second difference transformation.

The first and second difference of the spectrum iso-

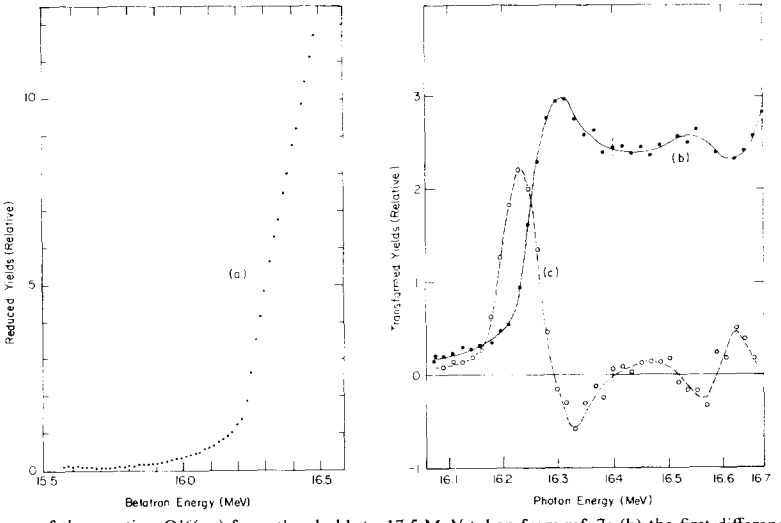

Fig. 2. (a) Yield curve of the reaction $O^{16}(\gamma n)$ from thresholds to 17.5 MeV taken from ref. 7; (b) the first difference of fig. 2a) with $\Delta = 68$ keV; (c) second difference of fig. 2(a) for $\Delta = 68$ keV.

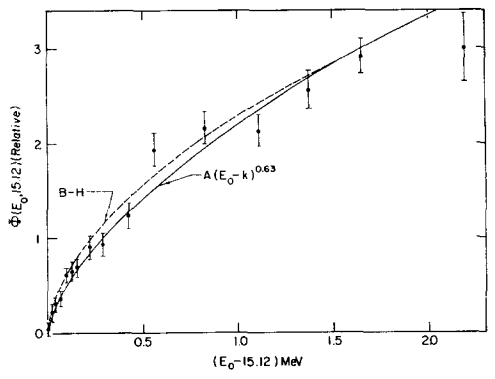

Fig. 3. Experimental bremsstrahlung isochromat obtained from the elastic scattering of 15.12 MeV photons from carbon. The dashed curve is the spectrum calculated from ref. 9.

chromat will lie intermediate between the weighting function shown in fig. 1 for $n = 0.5$ and 1.0. Since the isochromat represents the yield curve for a δ-function cross section, it is clear that the second difference of the isochromat closely approximates to the shape of the input cross section with two modifications. Firstly, the width of the peak in the s.d.w.f. shows the effect of the finite resolution of the method, and secondly, the negative overswing must be removed by an iterative procedure. (See eq. (13), sec. 3). The dashed curve in fig. 3 represents the isochromat at 15.12 MeV evaluated from the Bethe-Heitler bremsstrahlung cross section[9]) normalized to the experimental result at 16.5 MeV. The overall agreement of experiment with the Bethe-Heitler prediction is remarkably good.

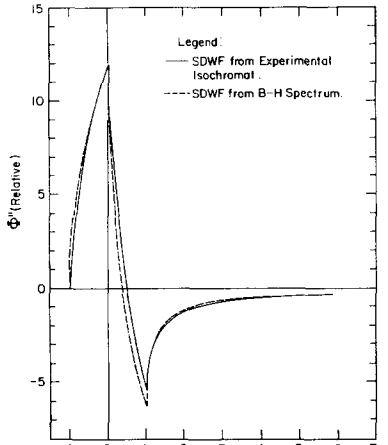

Fig. 4. Comparison of the s.d.w.f. obtained from the experimental determination shown in fig. 3 (solid curve) with that obtained from the spectrum calculated from ref. 9 (dashed curve).

Because of this agreement between our empirical isochromat and the Bethe-Heitler cross section, the latter is used to compute the s.d.w.f. In fig. (4) we compare the s.d.w.f. suggested by experiment (solid curve) with the Bethe-Heitler expression evaluated for $(E_0, \Delta) = (17.5, 0.068)$ MeV (dashed curve). The two curves are normalized at $E_0 - k = 0$. The difference between the two is not great; the Bethe-Heitler result gives a slightly larger negative overswing and a reduction in the low energy tail and has so far proved to be the most satisfactory s.d.w.f. for analysis.

The dependence of the s.d.w.f. on E_0 was investigated using the Bethe-Heitler expression for the bremsstrahlung intenstiy. For a given value of $(E_0 - k)/\Delta$ the absolute value of s.d.w.f. decrease monotonically with increasing E_0. A factor of 3 change in E_0 (10 to 30 MeV) changes s.d.w.f. by no more than 1% for all values of $(E_0 - k)/\Delta$. Therefore, the s.d.w.f. dependence on E_0 can be neglected without contributing a significant error to the computed cross section. Equation (12) is thus solved for $s(k)$ by an iteration procedure sliding the s.d.w.f. along the abscissa as E_0 is varied.

The dependence of s.d.w.f. on bin width, Δ, was also investigated using the Bethe-Heitler expression. At a given value of $(E_0 - k)/\Delta$, the absolute value of s.d.w.f. increases monotonically with increasing bin width. It is significant to note here that the behavior of the f.d.w.f. using the Bethe-Heitler expression, is just the converse, i.e. the low energy tail decreases with increasing bin width. This result is consistent with the empirical observation that the first difference of photonuclear yield curves over energy intervals of about 0.25–0.5 MeV closely resembles the actual cross section. Hence, the significance of the residual term in eq. (12) is reduced by taking the s.d.w.f. when $\Delta < 0.25$ MeV, whereas when $\Delta > 0.25$ MeV the f.d.w.f. is preferable. Application of the f.d.w.f. to an iterative solution of $s(k)$ from poor resolution photonuclear yield data ($\Delta = 0.5$MeV) was carried out by Carver and Lokan[11]).

4. Actual Calculational Procedure

4.1. Introduction

The statistical uncertainties inherent in experimental yields is reflected in the computed cross section, and is often responsible for excessive, non-physical oscillations of $s(k)$. Since both the actual $s(k)$ and the radiation spectrum are expected to be inherently continuous functions of the energy, the experimental data has been

[11]) J. H. Carver and K. Lokan, Aust. J. Physics **10** (1957) 312.

smoothed before attempting to compute $s(k)$. Smoothing of the experimental yield ordinates, whether subjectively by eye, or objectively by analytical procedures, damps out the non-physical oscillations with some sacrifice of energy resolution. In essence, smoothing the input data improves the real to spurious structure of the final result ("signal to noise ratio") by reducing the energy resolution (the "bandwidth"). Therefore, we have adopted the analytical smoothing procedure[12]) of piecewise least square fitting of the yield data over a limited energy interval.

4.2. Smoothing procedure applied to the present problem

In the present problem the yield data is fitted to a quartic function over an energy interval encompassed by 7 adjacent points ($M=7$). The order, n, of the fitting polynomial ($\Sigma a_n x^n$) and the fitting interval $(M-1)\Delta$ are not completely arbitrary, but related to the actual shape of the cross section. When sharp resonant structure is present in the cross section, then the quartic is a reasonable fitting function since it allows for points of inflection of the yield curve. The fitting interval determines the number of degrees of freedom $(M-n)$ and is selected to give an acceptable resolution. The general smoothing procedure is given in the appendix.

The s.d.w.f. and the corresponding smooth yield function, are each obtained as a linear combination of several $\Phi(k, E_0')$ and $y(E_0')$ respectively with coefficients given by the appropriate terms of the smoothing matrix. Specifically, for the problem at hand (see appendix, eq. (33)). The s.d.w.f. takes the form

$$\varphi''(k, E_0) = \frac{2}{\Delta^2} \sum_{m=1}^{1} \mathscr{S}_{3m} \Phi_m(k) \qquad (15a)$$

where $\Phi_m = \Phi(k, E_0 + (m-4)\Delta)$ and $\mathscr{S}_{3m}$ is obtained from table 2(a). Likewise, the second difference yield function is given by

$$\boldsymbol{y}''(E_0) = \frac{2}{\Delta^2} \sum_{m=1}^{7} \mathscr{S}_{3m} y_m \qquad (15b)$$

where

$$y_m = y\,[E_0 + (m-4)\Delta]$$

The s.d.w.f. evaluated for the Bethe-Heitler intensity distribution is shown in fig. 5 for $(E_0, \Delta) = (17.5, 0.068)$ MeV. This result does not differ significantly at the high energy tip from the s.d.w.f. obtained using the spectrum shape predicted by the empirical isochromat.

12) B. C. Cook, Phys. Rev. **106** (1957) 300.

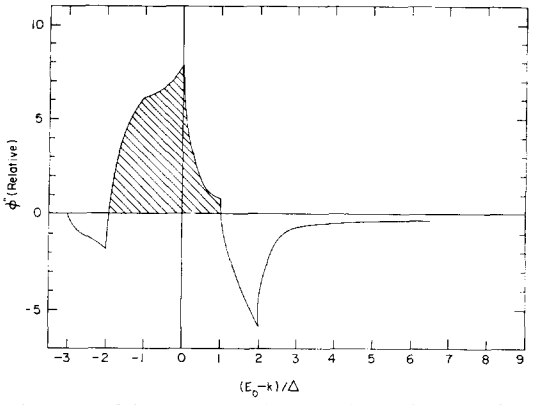

Fig. 5. S.d.w.f. for the Bethe-Heitler intensity distribution (ref. 9) for $(E_0,\Delta) = (17.5, 0.068)$ MeV with smoothing (7 points to a quartic function). The resolution function is shown as the shaded region.

The calculational procedure for $\overline{s(k)}$ is the same as before but with the transformed yield and spectrum replaced by their smoothed equivalents, (shown in bold face type). Equations (12) and (13) reduce to

$$\overline{s(k_t)} = s_0(E_0) - \int_0^{E_0'} \frac{dk}{\Delta} s(k) \boldsymbol{y}(k, E_0, \Delta) \qquad (16)$$

where

$$\overline{s(k)} = \int_0^{E_0'} dk s(k) \boldsymbol{\varphi}_t''(k, E_0)/\boldsymbol{w}(\Delta) \qquad (17a)$$

$$s(E_0) = \boldsymbol{y}''(E_0)/\boldsymbol{w}(\Delta) \qquad (17b)$$

$$\lambda(k, E_0, \Delta) = \boldsymbol{\varphi}_t''(k, E_0)\Delta/\boldsymbol{w}(\Delta) \qquad (17c)$$

$$\boldsymbol{w}(\Delta) = \int_0^{E_0'} \boldsymbol{\varphi}_t''(k, E_0)\, dk \qquad (17d)$$

and

$$E_0' = E_0 + \tfrac{1}{2}(M-1)\Delta \qquad (17e)$$

We select as our resolution function, $\varphi_t''(k, E_0)$, the s.d.w.f. contained in the interval $-2\Delta \leq E_0 - k \leq \Delta$ (see fig. 5, shaded region). The remainder of the (smooth) s.d.w.f. constitutes the residual weighting function $\lambda(k, E_0, \Delta)$.*

* A minor complication in computing with eq. (16) arises from the existence of the negative overswing in front of the resolution function (bin" − 3" in fig. 5). This is circumvented by setting up an iterative procedure such that on the first pass only, this bin is set to zero. On subsequent passes, therefore, there exists estimates of $s(k)$ for all k. The estimates for $s(k)$ rapidly converge and three of four passes suffice. This difficulty can be avoided by adopting for the smoothing procedure a five point fit to a cubic function (table 2b) instead of the seven point fit to a quartic function discussed in this paper.

Equation (16) is solved for $\overline{s(k)}$ by iteration. The integral term on the right side of this equation is replaced by its numerical equivalent $\Sigma_k \langle \overline{s(k)} \rangle \langle \lambda(k, E_0, \Delta) \rangle$ where $\langle s(k) \rangle$ and $\langle \lambda \rangle$ are the average values of the cross section and residual spectrum in the interval Δ. The energy corresponding to $\overline{s(k)}$ is given by the centroid of the resolution function, i.e. $k = E_0 + \frac{1}{2}\Delta$.

5. Test of the Method

As a consequence of choosing the s.d.w.f. as the transformed spectrum, it is found that the relative shape of the s.d.w.f. remains the same to within 1–2 percent as the peak energy E_0 is altered over a wide range, say 15–25 MeV. It is desirable to make an examination of the combined effect on the solution for the cross section of (a) the choice of s.d.w.f., its effective resolution function, and (b) the statistical variations of successive yield points and the possibility of generating spurious structure in the output data. Accordingly the following *thought-experiments* were devised.

Test 1. A (γ, n) cross section curve as a function of photon energy was obtained by adding four Breit-Wigner level cross sections whose parameters closely match those of the $O^{16}(\gamma, n)$ experimental data. The level parameters are listed in table 1. The curve so

TABLE 1
Level parameters chosen for imput cross section for test 1

Peak energy (MeV)	Peak cross section	Level width (MeV)
16.23	1.67	0.032
17.14	3.54	0.045
17.305	10.94	0.090
17.55	1.71	0.500

generated from threshold at 15.6 MeV to 18 MeV in 0.034 keV intervals is shown in fig. 6a.

Test 2. The input cross section, shown in fig. 6b, was taken as a parabola of the form $\sigma(E) = \varepsilon + 2\varepsilon^2$ where ε is equal to the difference between the photon energy E and the threshold, $E_T = 15.6$ MeV.

Test 3. A linear combination of the two input cross sections was taken to simulate a set of resonances with a continuum background and is shown in fig. 6c.

The corresponding yield curves are shown in fig. 7. These were generated from the respective cross sections according to the usual prescription as given by eq. (3) using the Bethe–Heitler bremsstrahlung spectrum[9]) which was calculated for each value of k and K_0. A set of yield curves typical of actual experiments were derived from those of fig. 7 by defining the statistical

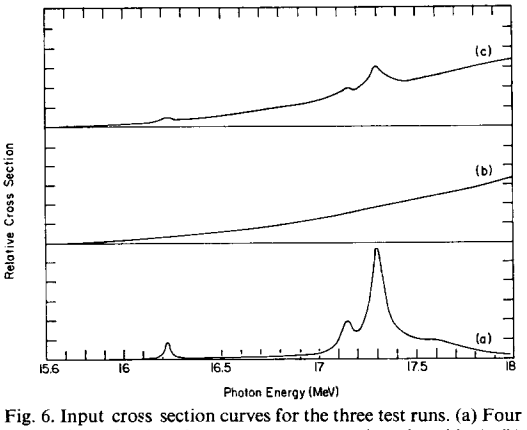

Fig. 6. Input cross section curves for the three test runs. (a) Four Breit-Wigner levels, whose parameters are given in table 1, (b) "continuum" cross section of parabolic form, (c) admitture of cross sections given in (a) and (b).

level of accuracy of, say, the highest energy point. This was taken at 300 000 counts throughout. Each yield point y_n was scaled up accordingly and its variance σ_n^2 was assumed equal to y_n, no other sources of variation being considered. For each simulated yield curve, a Monte Carlo method was used to compute the deviation $f_n\sigma_n$ of each yield point $y_n + f_n\sigma_n$ from the "true" yield y_n. A random number generator was used to select the magnitude and sign of f_n consistent with a normal error distribution. In this way a set of 6–10 completely independent yield curves embodying statistical fluctuations was generated for each test.

It is of incidental interest to observe the positions of "breaks" on these curves. In the favourable case of the

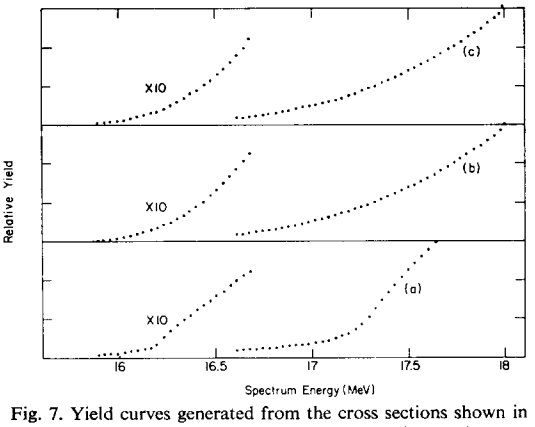

Fig. 7. Yield curves generated from the cross sections shown in fig. 6, (a) for test 1, (b) for test 2, and (c) for test 3.

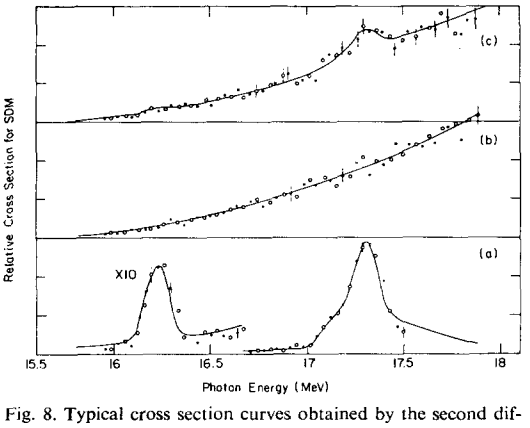

Fig. 8. Typical cross section curves obtained by the second difference method, (a) for test 1, (b) for test 2, and (c) for test 3. Each curve is obtained from the input cross section (fig. 6) convoluted with the s.d.w.f. resolution function. Solid error bars represent the standard error of the cross section obtained by propagating the variance through the second difference method. Dashed error bars represent the standard error obtained from the 6 to 10 independent yield curves.

first narrow level at 16.23, the break provides useful information. Such is not the case for the levels at 17.14, 17.31 MeV, and 17.5 MeV.

The yield curves were then analyzed by the s.d.m. yielding the result shown in fig. 8. Each cross section curve, it must be emphasized, was obtained with a s.d.w.f. compiled for only one value of K_0, viz. 17.51 keV, which was slid up or down. Resonance broadening of the cross section curves emerging from the s.d.m. shows the effect of the resolution of the method. This resolution function, shown in fig. 5, is convoluted with the input cross section to give the resultant curve shown in fig. 8. The agreement of the latter with the points from the s.d.m. is excellent.

The standard error computed by propagating the variance of each yield point through the various operations of the s.d.m. is shown for representative points by solid bars in fig. 8. On the other hand, external standard error computed from the dispersion of the analyzed cross sections for the 6–10 independent yield curves is shown by broken vertical lines on fig. 8. In general this latter error is less than, but not inconsistent with the former.

The results of test 1, confined to four levels only, indicate the satisfactory nature of the $\tilde{\Phi}_t$-portion (the resolution function) of s.d.w.f. for the analysis. Tests 2 and 3 show that the $\tilde{\Phi}_r$ portion of s.d.w.f. adequately predicts the cross section emerging from the s.d.m. since the $\tilde{\Phi}$ now has to operate on a sizeable cross section from threshold to the energy K_0. In fact, it adds an integrated weighted contribution of the cross section from threshold to K_0.

These three tests indicate the adequacy of s.d.m.

6. Photoneutron Cross Section for $O^{16}(\gamma, n)$

The s.d.m. has been successfully applied to analyse the $O^{16}(\gamma, n)$ cross section from 15.6 to 23 MeV. The results of the analysis from 18 to 23 MeV are shown in fig. 9. The smooth curve represents an analytical fit to the analysed cross section obtained by convoluting the s.d.w.f. resolution function with a linear superposition of Breit Wigner levels taken to synthesize the actual O^{16} (γ, n) cross section. Additional fine structure over that previously observed is accounted for by the improvement in the energy resolution of this method of analysis. The overall agreement with other obsrevations on O^{16} has been discussed in ref. 7.

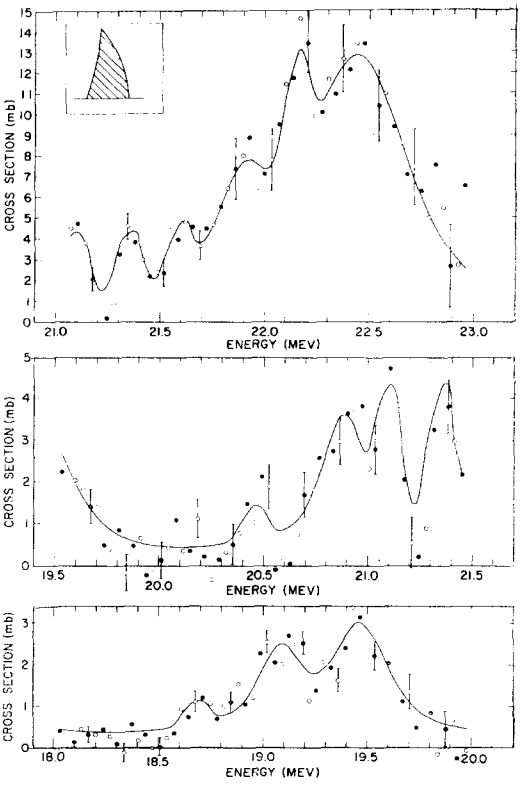

Fig. 9. Cross section for the $O^{16}(\gamma n)$ O^{15} reaction from 18 to 23 MeV. Analysis bin width, $\Delta E = 68$ keV. Resolution (see inset fwhm = 136 keV.

7. Conclusion

The s.d.m. for the analysis of bremsstrahlung yield curves has been shown to produce an effective cross section with energy resolution superior to any previous method. It has the advantages of having (1) a fairly well defined resolution function, and (2) of giving immediately in the second difference of the yield curve a good indication of the nature and type of resonant structure present. Computations were performed on an IBM 1620 computer without unduly long computing time.

Appendix

CALCULATION OF SMOOTHED SECOND DIFFERENCES OF THE YIELD AND SPECTRUM

A polynomial of degree n is piece-wise fitted to M yield ordinates where M is an odd integer, over a suitably chosen energy interval, symmetrically disposed about the central energy, E_0. The expression for the smoothed yield at some energy E_{0m} near E_0 is

$$Y(E_{0m}) = \sum_{j=0}^{n} \alpha_j(E_0)(E_0 - E_{0m})^j , \qquad (18)$$

where $E_0 - \frac{1}{2}d \leq E_{0m} \leq E_0 + \frac{1}{2}$d, and d is the smoothing interval. The $\alpha_j(E_0)$ are determined by a least squares analysis. When the yield ordinates are observed at equal energy intervals, Δ,

$$Y(E_{0m}) = \sum_{j=0}^{n} \alpha_j(E_0)\Delta^j \{ (E_0 - E_{0m})/\Delta \}^j . \qquad (19)$$

Equation (19) can be replaced by an equivalent expression in matrix representation which facilitates the general solution. Relative to the center energy E_0, the energy coordinates may be specified by the index m running from 1 to M, thus

$$\frac{E_0 - E_{0m}}{\Delta} = m - \frac{M+1}{2} \qquad (20)$$

and

$$Y(E_{0m}) \to Y_m . \qquad (21)$$

$M = d/\Delta + 1$ gives the number of ordinates to be fitted. Equation (19) is equivalent to

$$Y_m = \sum_{k=1}^{n+1} \beta_k \xi_{km} , \qquad (22)$$

where

$$\beta_k = \alpha_{k-1}(E_0)\Delta^{k-1}$$

and

$$\xi_{km} = (E_0 - E_{0m}/\Delta)^{k-1} = \{ m - \tfrac{1}{2}(M+1) \}^{k-1} . \qquad (23)$$

The β_k are obtained by the least square procedure of minimizing the sum of the squares of the ordinate deviations

$$\sum_{m=1}^{M} \left[y_m - \sum_{k=1}^{n+1} \beta_k \xi_{km} \right]^2 = \text{minimum} ,$$

where y_m is the reduced yield. The minimization process leads to a set of simultaneous equations

$$\sum_{m=1}^{M} \xi_{lm} y_m = \sum_{k=1}^{n+1} \beta_k R_{kl} , \qquad (24)$$

where the R matrix is defined by the direct product of the ξ matrix:

$$R_{kl} = \sum_{m=1}^{M} \xi_{km}\xi_{lm} = \sum_{m=1}^{M} \{ m - \tfrac{1}{2}(M+1) \}^{k+l-2} . \qquad (25)$$

The R matrix is a symmetric matrix of simple form with the following properties:

$$R_{kl} = 0 \text{ for } k + l \text{ odd} \qquad (26)$$

$$R_{kl} = 2 \sum_{v=0}^{\frac{1}{2}(M-1)} v^{k+l-2} \quad \text{for} \quad k + l \quad \text{even} . \qquad (27)$$

The solution of eq. (24) for β_k is straightforward;

$$\beta_k = \sum_{m=1}^{M} \mathscr{S}_{km} y_m \qquad (28)$$

where

$$\mathscr{S}_{km} = \sum_{l=1}^{M} R_{kl}^{-1} \xi_{lm} \qquad (29)$$

and is defined as the "smoothing matrix". From the definition of the R matrix, it immediately follows that

$$\sum_{m=1}^{M} \mathscr{S}_{km}\xi_{jm} = \delta_{jk} \text{ (Kronecker } \delta \text{ function)} . \qquad (30)$$

In terms of the $\mathscr{S}$ matrix

$$\alpha_{k-1}(E_0) = \frac{1}{\Delta^{k-1}} \sum_{m=1}^{M} \mathscr{S}_{km} y_m$$

$$= \frac{1}{\Delta^{k-1}} \sum_{m=1}^{M} \mathscr{S}_k(E_0, E_{0m}) y(E_{0m}) \qquad (31)$$

and the qth derivative of the yield function evaluated at E_0 is just $q!\alpha_q(E_0)$.

The smoothing matrices for $(M, n) = (7,4)$ and $(M, n) = (5,3)$ are given in table 2. The $(k-1)$ derivative of the smooth yield is obtained by taking the matrix product of the kth row of $\mathscr{S}$ with the column matrix y_m.

The integral equation (21) connecting the transformed yield, here taken as the second difference of the

TABLE 2(a)
Smoothing matrix $\mathscr{S}$ for $(M,n) = (7,4)$
(7 point fit to a quartic function)
$\mathscr{S}$ is defined by eq. (26)

0.0216450	−0.1298700	0.3246753	0.5670996	0.3246753	−0.1298700	0.0216450
0.0873016	−0.2658730	−0.2301587	0	0.2301587	0.2658730	−0.0873016
−0.0492425	0.2537878	−0.0719697	−0.2651514	−0.0719697	0.2537878	−0.0492425
−0.0277778	0.0277778	0.0277778	0	−0.0277778	−0.0277778	0.0277778
0.0113636	−0.0265151	0.0037879	0.0227273	0.0037878	−0.0265151	0.0113636

TABLE 2(b)
Smoothing matrix $\mathscr{S}$ for $(M,n) = (5,3)$

−0.0857143	0.3428571	0.4857143	0.3428571	−0.0857143
0.0833333	−0.6666667	0	0.6666667	−0.0833333
0.1428571	−0.0714286	−0.1428571	−0.714286	0.1428571
−0.0833333	0.1666667	0	−0.1666667	0.0833333

yield, to the spectrum is now replaced by the equivalent expression

$$y''(E_0) = \int_0^{E_0+\frac{1}{2}d} \mathrm{d}k s(k)\varphi''(k, E_0) \qquad (32)$$

where $\varphi''(k, E_0)$ is defined below. In terms of the smoothing matrix $\mathscr{S}$, $y''(E_0)$ is given by

$$y''(E_0) = \frac{2}{\Delta^2} \sum_{m=1}^{M} \mathscr{S}_{3m} y_m$$

which in terms of eq. (31) gives

$$y''(E_0) = \frac{2}{\Delta^2} \sum_{E_0'=E_0-\frac{1}{2}d}^{E_0+\frac{1}{2}d} \mathscr{S}_3(E_0, E_0') y(E_0') . \qquad (33)$$

The smoothed second difference of the spectrum is computed using the same smoothing procedure. Replacing y_m by the target spectrum $\Phi_m(k)$, eq. (33) gives for the s.d.w.f.,

$$\varphi''(k, E_0) = \frac{2}{\Delta^2} \sum_{m=1}^{M} \mathscr{S}_{3m} \Phi_m(k) \qquad (34)$$

$$\frac{2}{\Delta^2} \sum_{m=1}^{M} \mathscr{S}_3(E_0, E_0') \Phi(k, E_0') .$$